Available online at www.sciencedirect.com

ScienceDirect

Ceramics International 40 (2014) 17–23

CERAMICS INTERNATIONAL

www.elsevier.com/locate/ceramint

Microstructure evolution and its effect on the mechanical properties of the ZrC–SiC composite joint diffusion bonded with pure Ni foil

Changbao Song[a], Tiesong Lin[a], Peng He[a,*], Weiqi Yang[a], Dechang Jia[b], Jicai Feng[a]

[a]State Key Laboratory of Advanced Welding and Joining, Harbin institute of Technology, Harbin 150001, China
[b]Institute for Advanced Ceramics, Harbin Institute of Technology, Harbin 150001, China

Received 30 September 2012; received in revised form 21 April 2013; accepted 22 April 2013
Available online 27 April 2013

Abstract

The ZrC—20 vol% SiC composite was diffusion bonded with pure Ni foil as the interlayer. The interfacial microstructure evolution and its effect on the mechanical property of the joint were investigated. The results showed that Ni reacted preferentially with SiC. The corresponding reaction products were Ni_2Si and C. During longer holding time or at higher joining temperature, the reaction product Ni_2Si separated from C and penetrated along ZrC boundaries. Meanwhile, C transformed into pieces of graphite. Beside the ZrC/Ni interface, nickel based solid solution and fine graphite were observed due to the slight reaction between ZrC and Ni. With increasing in joining temperature, Ni was consumed gradually and the transition layer increased in thickness. The shear strength of the joints increased to the maximum and then decreased with increasing joining temperature from 800 °C to 1200 °C. The maximal value of 168 MPa was obtained when joined at 1000 °C under 20 MPa for 30 min.

Keywords: A. Joining; B. Microstructure; C. Mechanical properties; D. ZrC–SiC composite

1. Introduction

ZrC–SiC composites have drawn increasing attention in recent years for their excellent properties [1,2]. When compared with pure ZrC ceramic, which is an important family member of ultrahigh-temperature ceramics (UHTCs), the ZrC–SiC composites show a better combination of sinterability, oxidation resistance and mechanical properties [3–6]. However, like most engineering ceramics, ZrC–SiC composites are brittle, making it difficult to obtain large-sized or complex components. Therefore, joining of ZrC–SiC composites to themselves or to metals becomes a promising way when put them into application. Unfortunately, the reports on ZrC–SiC composites are mainly about their preparation [7–10], while little work has been reported on their joining by far.

In the joining of ceramics or ceramics and metals, active metal brazing is an efficient technology [11–14]. Especially, a large number of active metal alloys containing Ti element such as Ag–Cu–Ti [15], Ti–Cu [16] and Ti–Zr–Ni–Cu [17] have been successfully developed. Taking SiC for example, high quality joints can be obtained when brazed with these active metal alloys. The representative microstructure of these brazed joints is a reaction layer composed of TiC and Ti_5Si_3 at the SiC/brazing seam interface [18]. The thickness of the reaction layer is crucial to their mechanical properties. Thickening in the reaction layer increases mismatch of coefficients of thermal expansion (CET) between SiC substrate and the reaction layer. Consequently, high residual stresses lead to poor mechanical properties. Crucially, the joints cannot serve at high temperature environment due to the relative low melting temperatures of those active filler metals. Therefore, more attention has been focused on other high temperature brazing filler metals, such as Ni-based [19–21], Co-based [22] and even Au-based [23] or Pd-based brazing fillers [24]. For example, a CoFeNi(Si, B) CrTi filler metal has been reported in the joining of SiC to nickel-based super alloy for high temperature application [25]. The achieved SiC–SiC joints showed excellent mechanical properties when brazed at 1150 °C for 10 min with rapidly-solidified CoFeNi(Si,B)CrTi foil. To obtain sound SiC–metal joints, a Ni foil was used as the buffer interlayer to relax the residual thermal stresses. Unfortunately, excessive reaction occurred between Ni and SiC due to the dissolution of Ni

*Corresponding author. Tel./fax: +86 451 8640 2787.
E-mail addresses: hithepeng@hit.edu.cn, hepeng@hit.edu.cn (P. He).

0272-8842/$ - see front matter © 2013 Elsevier Ltd and Techna Group S.r.l. All rights reserved.
http://dx.doi.org/10.1016/j.ceramint.2013.04.074

interlayer in the molten CoFeNi(Si,B)CrTi filler metal. Finally, the joints cracked in the reaction layer near the SiC/brazing seam interface.

Among all above-mentioned high temperature brazing filler metals, Ni is one of the most important active constituents due to its relatively high melting temperature, low vapor pressure and good ductility. Ni is also considered as an ideal interlayer in diffusion bonding of ZrC–SiC composite to obtain high temperature joints [26–29]. Up to now, some reports have discussed about the interaction in Ni–SiC system [30–33]. In the wetting experiments obtained by the sessile drop method, the contact angles of pure Ni on SiC substrate lies between 50° and 75° [34,35]. Usually, the wetting is accompanied by a high reactivity, including dissolution of SiC and precipitation of large graphite lamellas [36]. Similar reactions take place in the solid state reaction between Ni and SiC [37,38]. In brief, the elements Ni and Si have strong affinity with each other. The interaction products, including Ni silicides and graphite, bring about dangerous brittleness. In Ni–ZrC system, the interfacial reaction has been studied in the joining experiment of ZrC with Ni/Nb/Ni interlayer [39]. The Ni–ZrC interaction products are Ni–Zr compounds and graphite. Nevertheless, the reaction between Ni and ZrC is not as strong as that in Ni–SiC system.

As analyzed above, the violent Ni–SiC interaction appears to be unfavorable to the joints. However, the volume of SiC in the ZrC–SiC composite used in this study is only 20%. So the discontinuous interfacial reaction between SiC and Ni will form an "anchor structure", which is beneficial to the mechanical properties of the joints [40]. Although Ni reacts with both ZrC and SiC, the interaction mechanism of ZrC–SiC/Ni system needs further study. Especially, the effect of Ni–SiC interaction on the mechanical properties of the ZrC–SiC composite joint is not clear at present, which is indeed the objective of the present study.

2. Experimental procedure

The ZrC—20 vol% SiC composite (ZS) was fabricated by hot pressing at 2000 °C for 60 min under a pressure of 30 MPa. Commercial ZrC and SiC powders were used as the starting materials. The sizes of the powders are both about 2 μm. The relative density of the prepared ZS composite reaches 97%. The microstructure of the composite is shown in Fig. 1. The ZS composite was sliced into 5 mm × 5 mm × 3 mm pieces for the metallographic observation and shear test. Pure Ni foil with a thickness of 50 μm was used as the interlayer in this study.

Prior to the joining procedure, the contact surfaces of ZS composite pieces were polished by diamond grinding discs up to 1200-grit. All the joining ZS composite pieces and Ni foil were ultrasonically cleaned in acetone for 15 min. The joining samples, assembled in the order of ZS/Ni/ZS (shown in Fig. 2 (a)), were put into a vacuum furnace with a vacuum of 1×10^{-3} Pa. The pressure applied on the samples was 20 MPa. The samples were heated to 750 °C with a heating rate of 30 °C min^{-1} and then held for 5 min. After that, the samples were further heated to joining temperatures (800–1200 °C) with a heating rate of 15 °C min^{-1} and then isothermally held for 30 min. In the cooling stage, the samples

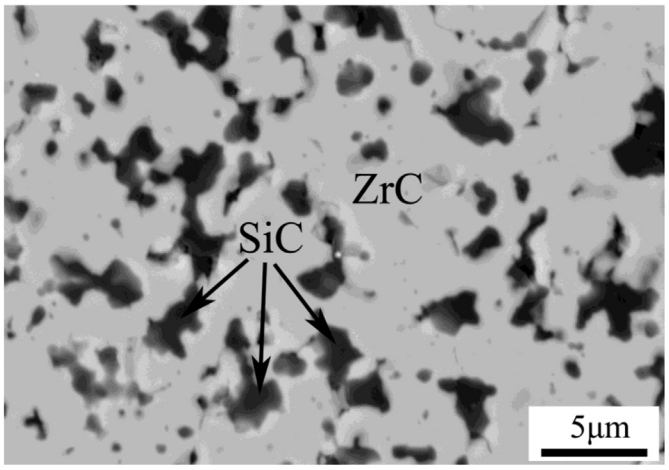

Fig. 1. Backscattered electron image of the ZrC—20 vol% SiC composite.

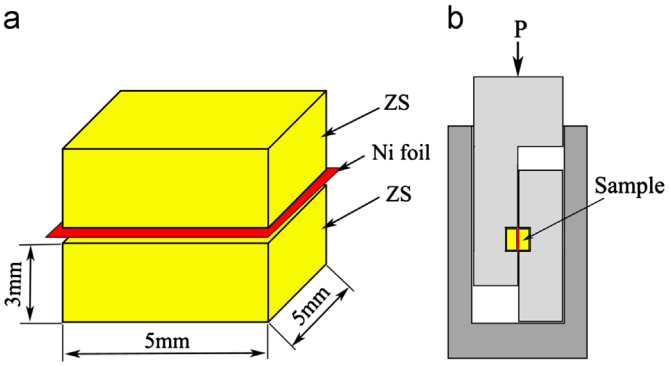

Fig. 2. (a) Assemblage of the sample and (b) shear test apparatus.

were cooled to 450 °C with a rate of 5 °C min^{-1}, and then followed by furnace cooling to room temperature.

Cross-sectional specimens of the bonded joints were prepared with the conventional mechanical polishing method for microstructural observations. On the surface of those polished specimens, the transmission electron microscope (TEM) specimens were prepared by a focus ion beam (FIB) micro sampling method with HELIOS NanoLab 600i (FEI Co., Ltd., USA). The microstructural observations were carried out with scanning electron microscopy (Quanta 200FEG, FEI Co., Ltd.) equipped with energy dispersive X-ray spectroscopy (EDS, AMETEK). The TEM observations were performed with Tecnai G2 F30 (FEI Co. Ltd.). Phase compositions of the reaction products were analyzed by selected area electron diffraction (SAED) patterns. The shear strength of the joints was tested using the Instron-1186 universal testing machine, as shown in Fig. 2(b).

3. Results and discussion

3.1. Interfacial structure analysis of ZS/Ni/ZS joint

Fig. 3 shows the typical cross-section microstructure of the ZS/Ni/ZS joint. The joint was bonded at 900 °C for 30 min under a pressure of 20 MPa.

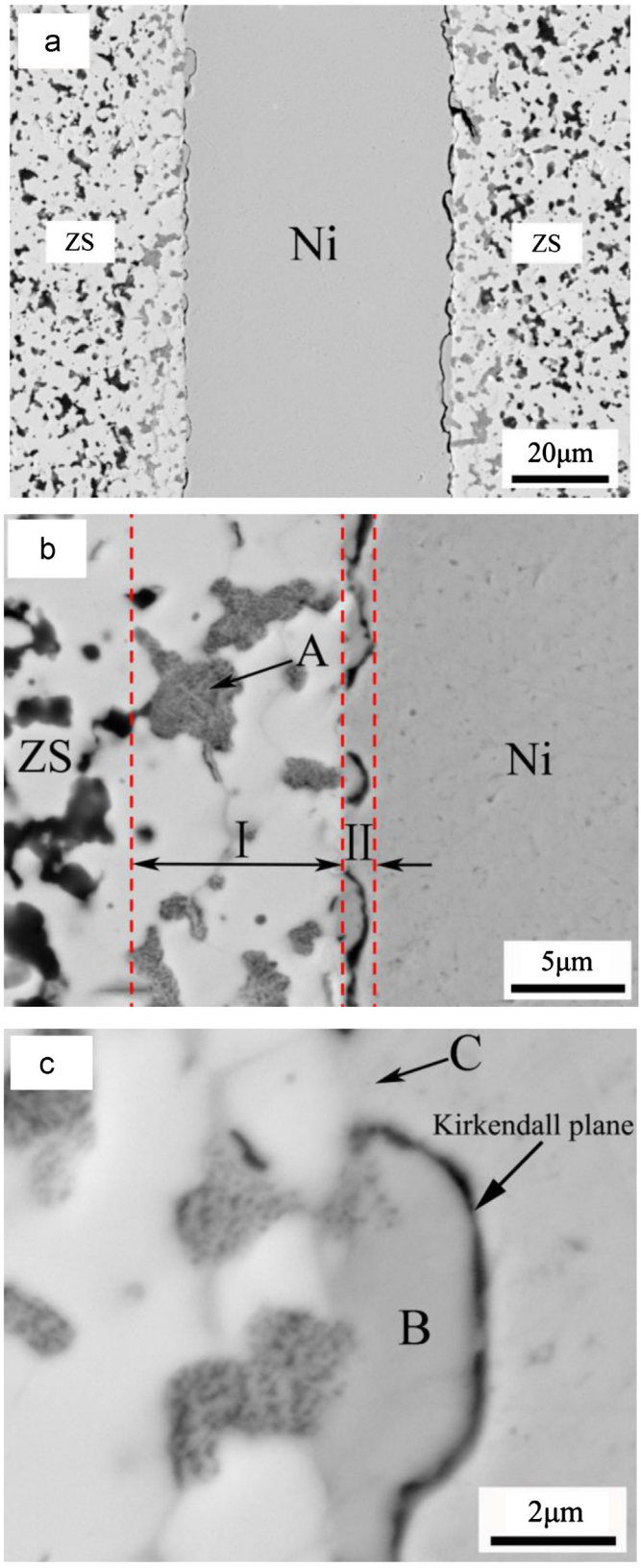

Fig. 3. Backscattered electron images of ZS/Ni/ZS joint (900 °C/30 min/20 MPa): (a) microstructure of the joint; (b) and (c) magnification of the interface.

A general observation in Fig. 3 confirms the interaction between ZS composite and Ni interlayer. It is notable that several products have formed near the interface. The chemical compositions of the reaction phases A–C were measured by EDS. The results are shown in Table 1. As shown in Fig. 3(b), two characteristic layers have formed at each side of the interface: (I) transition layer in ZS composite, and (II) a discontinuous layer near the Ni interlayer. The transition layer is about 10 μm in width. In the transition layer, the black SiC particles were consumed during the interaction and replaced by the netlike reaction products. However, the reaction products near the Ni interlayer are not continuous. Lots of fan-shaped bulks are separated from the Ni interlayer by gaps. These gaps are, in fact, symbols of Kirkendall planes [27].

According to the EDS analysis results, the netlike reaction products, locating at the places where SiC particles once occupied, are composed of Ni, Si and C. The ratio of Ni to Si is about 2:1. The possible phases are Ni_2Si and graphite. The remaining two phases, labeled as B and C in Fig. 3(c), are inferred to be a kind of Ni silicide and Ni-based solid solution, respectively. A further study of TEM observation was performed for a better understanding of the reaction in Ni–ZS system.

The TEM observation region was vertical to the interface, including part of the transition layer and Ni interlayer. The morphologies of different phases and corresponding SAED patterns are shown in Figs. 4 and 5, respectively. As shown in Fig. 4, the Ni–SiC reaction products in the transition layer were proved to be Ni_2Si and graphite. The SiC particle was replaced by a mixture of the gray Ni_2Si and white graphite. Besides, a portion of Ni_2Si separated from graphite and spread along the ZrC grain boundaries.

Fig. 5 shows the typical bright field (BF) image of the Ni–ZS interface. Near the Ni/SiC interface, a mixture of Ni_2Si and graphite distribute in the transition layer. The Kirkendall pore can be clearly observed at the interface. However, the dark phase around the Kirkendall pore was detected as a kind of amorphous material according to the SAED pattern. That is to say, the Ni silicide near the pore was not successfully observed in this specimen and further study is needed. The Ni/ZrC interface is relatively smooth and some fine graphite distributes along the Ni/ZrC interface. However, about 5 at% Zr was detected in the Ni interlayer near the interface by EDS analysis, as shown in Fig. 6. The EDS results reveal that slight reaction has happened between Ni and ZrC. The corresponding reaction products are graphite and Ni-based solid solution.

Ni reacts with both SiC and ZrC but at different reaction levels. Accordding to the experimental results, the interaction between Ni and SiC is far more rapid and violent. This is caused by the strong affinity between the two elements Ni and Si.

Table 1
The EDS results of different points at the interface (at%).

Points	Zr	Si	C	Ni	Possible phases
A	2	11	66	21	Ni_2Si+C
B	1	30	–	69	Ni-silicide
C	1	–	1	98	Ni (s, s)

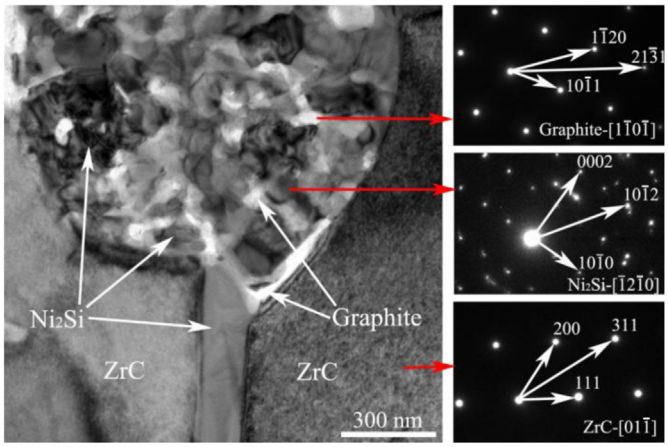

Fig. 4. Bright field image of the transition layer and corresponding SAED patterns.

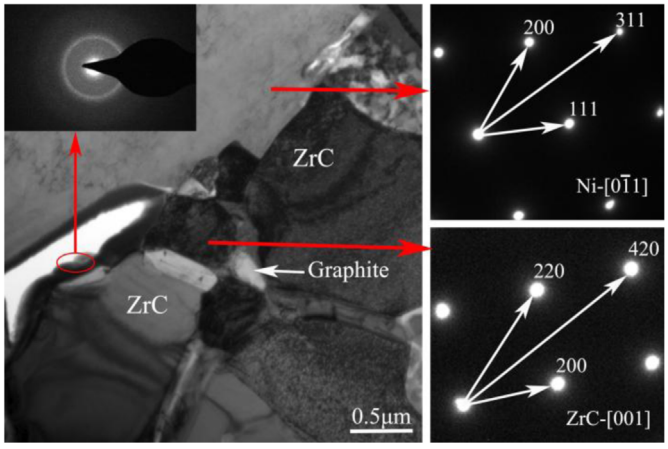

Fig. 5. Bright field image of Ni/ZS interface and SAED patterns of different phases.

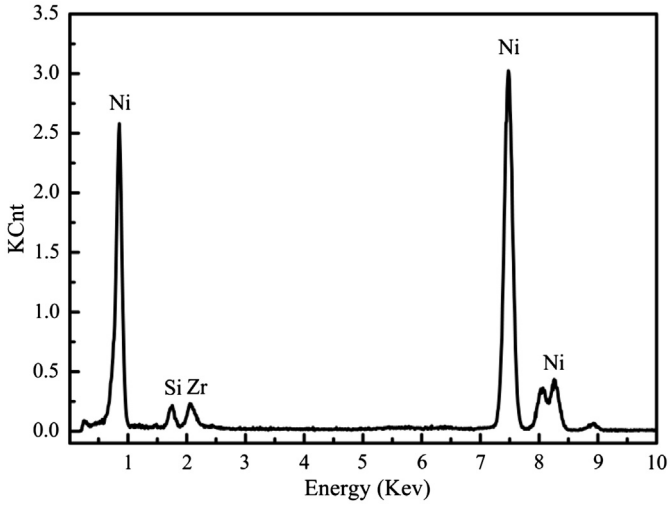

Fig. 6. EDS results obtained in the Ni interlayer near Ni/ZrC interface.

In Ni–SiC reaction system, the possible products NiSi, Ni_2Si and Ni_3Si are all thermodynamically stable under the present experimental conditions. However, Ni_2Si and Ni_3Si are the most probable products because the ΔG values are highly negative. They are -46 KJ mol^{-1} and -43.8 KJ mol^{-1} at 900 °C. According to the experimental results, Ni reacted preferentially with SiC particles once the interlayer got in touch with ZS composite. Theoretically, Ni_2Si should appear at the SiC side and more Ni-rich Ni_3Si should form near the Ni interlayer. In practice, Ni_2Si was observed in the transition layer while Ni_3Si was difficult to be observed under such an nonequilibrium diffusion state. Factually, the formation of Ni_3Si would result in a row of pores at the Ni_3Si/Ni interface due to the different diffusion velocities of Ni and Si in Ni–Si compounds. Ni diffuses one or two orders of magnitude faster than Si in Ni_3Si, which leads to the formation of pores at the Ni_3Si/Ni interface [27]. The pores connect each other gradually and thus transform into gaps during the reaction process, as shown in Fig. 3(c). Once the transport of Ni is hindered by the formed gaps, the consumption of Ni_3Si starts, which is in favor of the growth of other Si-rich phases, Ni_5Si_2 or even Ni_2Si, for example. In these cases, the Ni/SiC diffusion couples become in fact Ni_3Si/SiC or Ni_5Si_2/SiC diffusion couples. During the joining with higher temperature or longer holding time, the Ni_3Si phase will be partly consumed by the neighboring phase. Therefore, the Ni silicide near the Kirkendall pores would be Ni_3Si. But it is possible that the Ni silicide has partly transformed into Ni_5Si_2 or even Ni_2Si.

3.2. Microstructure evolution of ZS/Ni/ZS joint

Fig. 7 shows the interfacial microstructure of the ZS/Ni/ZS joints diffusion bonded at different temperatures. The joint thickened in transition layer while Ni interlayer was gradually consumed at higher joining temperature. When the joining temperature increased from 900 °C to 1000 °C, the thickness of the transition layer increased from 10 μm to about 40 μm, as shown in Fig. 7(a). The morphologies and distribution of the reaction products also changed. Separation of the reaction products became quite distinct. More and more Ni_2Si spread along the ZrC grain boundaries while large pieces of graphite was left behind, as shown in Fig. 7(b).

When the joint was bonded at 1100 °C under 20 MPa for 30 min, the Ni foil was completely consumed during the interaction. Homogenous joints were obtained under the given joining conditions, as shown in Fig. 7(c). The whole thickness of the transition layer reached 300 μm and the graphite has grown into large lamellas, as shown in Fig. 7(d).

3.3. Mechanical property of ZS/Ni/ZS joint

Mechanical property of the ZS/Ni/ZS joints was evaluated by shear test. The results are shown in Fig. 8. The testing diagram in Fig. 2(b) shows how the load is applied. The average strength is evaluated from five test values. The error bars show the fluctuations when compared with the average values. The shear strength increases to the maximum and then decreases with increasing joining temperature from 800 °C to 1200 °C. The maximal value reaches 168 MPa at 1000 °C.

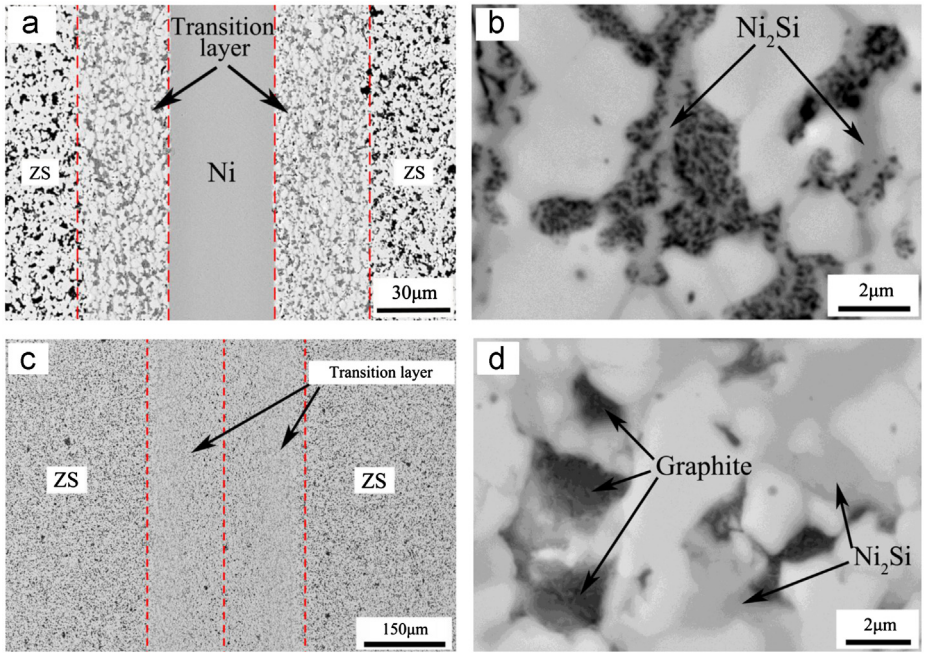

Fig. 7. Microstructures of the ZS/Ni/ZS joints bonded at different temperatures: (a) joint bonded at 1000 °C and (b) magnification of the transition layer; (c) joint bonded at 1100 °C and (d) magnification of the transition layer.

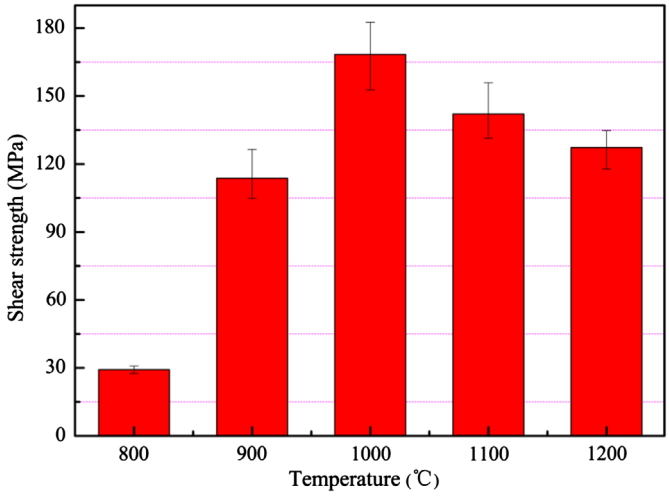

Fig. 8. The effect of joining temperature on the shear strength of ZS/Ni/ZS joints.

The evolution in microstructure of the ZS/Ni/ZS joints has a decisive effect on the shear strength. Variation in the shear strength can be explained as follows. When the joining temperature was relatively low, taking 900 °C for example, the reaction at the Ni/ZS interface was weak. Large amount of pores were observed at the Ni/ZS interface, as shown in Fig. 3. The Kirkendall pores or planes formed near the interface weakened the strength of the joints, leading to a relative low shear strength. As a result, the fracture of the joint was relatively smooth, as shown in Fig. 9(a) and (d).

The increasing in joining temperature promotes the interfacial reaction between ZS composite and Ni interlayer. In particular, the disappearance of Kirkendall pores or gaps is beneficial to the mechanical property of the joints. When the joining temperature is increased to 1000 °C, the joints had a mixed fracture mode. Most of the fracture path was in the transition layer according to the reaction products detected on the fracture surface, as shown in Fig. 9(b) and (e). Nevertheless, the fracture was uneven and the crack propagated partially in the ZS composite. Correspondingly, the maximal shear strength of 168 MPa was obtained. When the joining temperature continued to increase, large pieces of graphite were formed in the joints (shown in Fig. 9(c) and (f)). The formed graphite brought about harmful brittleness to the joints and lead to a decrease in the shear strength.

4. Conclusions

The ZS composite was successfully joined with pure Ni foil as the interlayer. Based on the results obtained in this study, the conclusions can be summarized as follows:

(1) The interfacial reaction between Ni and ZS composite focuses on the Ni–SiC system. Corresponding reaction products are Ni_2Si and C. The relatively weak Ni–ZrC reaction produces C and Ni based solid solution.
(2) The thickness of the transition layer increased with increasing in the joining temperature. A portion of Ni_2Si spread along the ZrC grain boundaries, while C transformed into large pieces of graphite.
(3) The shear strength of the joints increased to the maximum and then decreased when the joining temperature increased from 800 °C to 1200 °C. The maximal shear strength of 168 MPa was obtained when joined at 1000 °C for 30 min under 20 MPa.

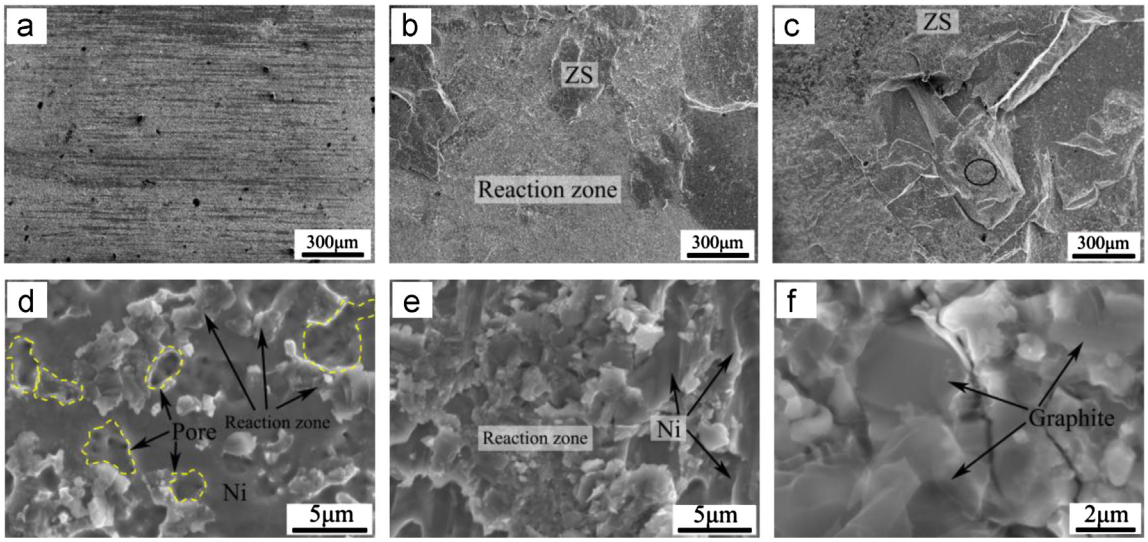

Fig. 9. The fracture of the joints obtained at different temperatures: (a), (b) and (c) fracture of the joint bonded at 900 °C, 1000 °C and 1100 °C respectively; (d), (e) and (f) magnification of the reaction area in (a), (b) and (c).

Acknowledgments

The authors gratefully acknowledge the financial support from the National Natural Science Foundation of China (Grant nos. 50975062, 51105107 and 51021002), the Natural Science Foundation of Heilongjiang Province (Grant no. QC2011C044) and the Specialized Research Fund for the Doctoral Program of Higher Education (Grant no. 20112302130005).

References

[1] D. Pizon, R. Lucas, S. Chehaidi, S. Foucaud, A. Maitre, From trimethylvinylsilane to ZrC–SiC hybrid materials, Journal of the European Ceramic Society 31 (2011) 2687–2690.
[2] Qinggang Li, Haijun Zhou, Shaoming Dong, Zhen Wang, Ping He, Jinshan Yang, Bin Wu, Jianbao Hu, Fabrication of a ZrC–SiC matrix for ceramic matrix composites and its properties, Ceramics International 38 (2012) 4379–4384.
[3] Liyou Zhao, Dechang Jia, Xiaoming Duan, Zhihua Yang, Yu Zhou, Oxidation of ZrC—30 vol% SiC composite in air from low to ultrahigh temperature, Journal of the European Ceramic Society 32 (2012) 947–954.
[4] Yang Xiang, Wei Li, Song Wang, Zhaohui Chen, Ablative property of ZrC–SiC multilayer coating for PIP-–C/SiC composites under oxy-acetylene torch, Ceramics International 38 (2012) 2893–2897.
[5] Baoxia Ma, Wenbo Han, Thermal shock resistance of ZrC matrix ceramics, International Journal of Refractory Metals and Hard Materials 28 (2010) 187–190.
[6] Sean E. Landwehr, Gregory E. Hilmas, William G. Fahrenholtz, Inna G. Talmy, Stephen G. Dipietro, Microstructure and mechanical characterization of ZrC–Mo cermets produced by hot isostatic pressing, Materials Science and Engineering A 497 (2008) 79–86.
[7] Liyou Zhao, Dechang Jia, Xiaoming Duan, Zhihua Yang, Yu Zhou, Low temperature sintering of ZrC–SiC composite, Journal of Alloys and Compounds 509 (2011) 9816–9820.
[8] Bharat P. Das, M. Panneerselvam, K.J. Rao, A novel microwave route for the preparation of ZrC–SiC composites, Journal of Solid State Chemistry 173 (2003) 196–202.
[9] B. Ma, X. Zhang, J. Han, W. Han, Fabrication of hot-pressed ZrC-based composites, Proceedings of the Institution of Mechanical Engineers, Part G: Journal of Aerospace Engineering 223 (2009) 1153–1157.
[10] Liyou Zhao, Dechang Jia, Xiaoming Duan, Zhihua Yang, Yu Zhou, Pressureless sintering of ZrC-based ceramics by enhancing powder sinterability, International Journal of Refractory Metals and Hard Materials 29 (2011) 516–521.
[11] Gurdial Blugan, Jakob Kuebler, Vinzenz Bissig, Jolanta Janczak-Rusch, Brazing of silicon nitride ceramic composite to steel using SiC-particle reinforced active brazing alloy, Ceramics International 33 (2007) 1033–1039.
[12] Jiake Li, Lei Liu, Yating Wu, Zhibin Li, Wenlong Zhang, Wenbin Hu, Microstructure of high temperature Ti-based brazing alloys and wettability on SiC ceramic, Materials and Design 30 (2009) 275–279.
[13] W.B. Hanson, K.I. Ironside, J.A. Fernie, Active metal brazing of zirconia, Acta Materialia 48 (2000) 4673–4676.
[14] O. Kozlova, M. Braccini, R. Voytovych, N. Eustathopoulos, P. Martinetti, M.F. Devismes, Brazing copper to alumina using reactive CuAgTi alloys, Acta Materialia 58 (2010) 1252–1260.
[15] Jinhui Xiong, Jihua Huang, Hua Zhang, Xingke Zhao, Brazing of carbon fiber reinforced SiC composite and TC4 using Ag–Cu–Ti active brazing alloy, Materials Science Engineering A 527 (2010) 1096–1101.
[16] Xing Wang, Laifei Cheng, Shangwu Fan, Litong Zhang, Microstructure and mechanical properties of the GH783/2.5D C/SiC joints brazed with Cu–Ti+Mo composite filler, Materials and Design 36 (2012) 499–504.
[17] E. Ganjeh, H. Sarkhosh, M.E. Bajgholi, H. Khorsand, M. Ghaffari, Increasing Ti–6Al–4V brazed joint strength equal to the base metal by Ti and Zr amorphous filler alloys, Materials Characterization 71 (2012) 31–40.
[18] Y. Liu, Z.R. Huang, X.J. Liu, Joining of sintered silicon carbide using ternary Ag–Cu–Ti active brazing alloy, Ceramics International 35 (2009) 3479–3484.
[19] Z.W. Yang, L.X. Zhang, P. He, J.C. Feng, Interfacial structure and fracture behavior of TiB whisker-reinforced C/SiC composite and TiAl joints brazed with Ti–Ni–B brazing alloy, Materials Science Engineering A 532 (2012) 471–475.
[20] G.W. Liu, F. Valenza, M.L. Muolo, G.J. Qiao, A. Passerone, Wetting and interfacial behavior of Ni–Si alloy on different substrates, Journal of Materials Science 44 (2009) 5990–5997.
[21] G.W. Liu, F. Valenza, M.L. Muolo, A. Passerone, SiC/SiC and SiC/Kovar joining by Ni–Si and Mo interlayers, Journal of Materials Science 45 (2010) 4299–4307.
[22] Huaping Xiong, Xiaohong Li, Wei Mao, Yaoyong Cheng, Wetting behavior of Co based active brazing alloys on Si and the interfacial reactions, Materials Letters 57 (2003) 3417–3421.

[23] M. Singh, T.P. Shpargel, R. Asthana, Brazing of stainless steel to yttria-stabilized Zirconia using gold-based brazes for solid oxide fuel cell application, International Journal of Applied Ceramic Technology 4 (2007) 119–133.
[24] R. Asthana, M. Singh, Joining of ZrB_2-based ultra-high-temperature ceramic composites using Pd-based braze alloys, Scripta Materialia 61 (2009) 257–260.
[25] Hua Ping Xiong, Wei Mao, Yong Hui Xie, Wan Lin Guo, Xiao Hong Li, Yao Yong Cheng, Brazing of SiC to a wrought nickel-based superalloy using CoFeNi(Si, B)CrTi filler metal, Materials Letters 61 (2007) 4662–4665.
[26] Zhihong Zhong, Hun-chea Jung, Tatsuya Hinoki, Akira Kohyama, Effect of joining temperature on the microstructure and strength of tungsten/ferritic steel joints diffusion bonded with a nickel interlayer, Journal of Materials Processing Technology 210 (2010) 1805–1810.
[27] Zhihong Zhong, Tatsuya Hinoki, Hun-chea Jung, Yi-Hyun Park, Akira Kohyama, Microstructure and mechanical properties of diffusion bonded SiC/steel joint using W/Ni interlayer, Materials Design 31 (2010) 1070–1076.
[28] M.I. Osendi, A. De Pablos, P. Miranzo, Microstructure and mechanical strength of Si_3N_4/Ni solid state bonded interfaces, Materials Science and Engineering A 308 (2001) 53–59.
[29] M.L. Hattali, S. Valette, F. Ropital, N. Mesrati, D. Tréheux, Interfacial behavior on Al_2O_3/HAYNES 214™ joints fabricated by solid state bonding technique with Ni or Cu–Ni–Cu interlayers, Journal of the European Ceramic Society 32 (2012) 2253–2265.
[30] Jan H. Gülpen, Alexander A. Kodentsov, Frans J.J. van Loo, Growth of silicides in Ni–Si and Ni–SiC bulk diffusion couples, Zeitschrift fur Metallkunde 86 (1995) 530–539.
[31] A. Hahnel, E. Pippel, J. Woltersdorf, Control of Ni/SiC reactions by germanium, studied on the atomic scale, Scripta Materialia 60 (2009) 858–861.
[32] M.L Hattali, S. Valette, F. Ropital, G. Stremsdoerfer, N. Mesrati, D. Tréheux, Study of SiC–nickel alloy bonding for high temperature applications, Journal of the European Ceramic Society 29 (2009) 813–819.
[33] G.A. Yasinskaya, The wetting of refractory carbides, borides and nitrides by molten metals, Powder Metallurgy and Metal Ceramics 7 (1966) 557–559.
[34] P. Nikolopoulos, S. Agathopoulos, G.N. Angelopoulos, A. Naoumidis, H. Grübmeier, Wettability and interfacial energies in SiC–liquid metal systems, Journal of Materials Science 27 (1992) 139–145.
[35] G.W. Liu, M.L. Muolo, F. Valenza, A. Passerone, Survey on wetting of SiC by molten metals, Ceramics International 36 (2010) 1177–1188.
[36] C. Rado, S. Kalogeropoulou, N. Eustathopoulos, Wetting and bonding of Ni–Si alloys on silicon carbide, Acta Materialia 46 (2) (1999) 461–473.
[37] R.C.J. Schiepers, J.A. Van Beek, F.J.J. Van Loo, G. De With, The interaction between SiC and Ni, Fe, (Fe, Ni) and steel: morphology and kinetics, Journal of the European Ceramic Society 11 (1993) 211–218.
[38] Y. Cao, L. Nyborg, D.Q. Yi, U. Jelvestam, Study of reaction process on Ni/4H–SiC contact, Materials Science Technology 22 (10) (2006) 1227–1234.
[39] Laura Silvestroni, Diletta Sciti, Laura Esposito, Aandreas M. Glaeser, Joining of ultra-refractory carbides, Journal of the European Ceramic Society 32 (2012) 4469–4479.
[40] Bo Yuan, Guo-Jun Zhang, Microstructure and shear strength of self-joined ZrB_2 and ZrB_2–SiC with pure Ni, Scripta Materialia 64 (2011) 17–20.